Zygote **7** (August), pp 211–222. © 1999 Cambridge University Press Printed in the United Kingdom

Hyaluronic acid and the cumulus extracellular matrix induce increases in intracellular calcium in macaque sperm via the plasma membrane protein PH-20

Gary N. Cherr[1], *Ashley I. Yudin*[2], *Ming-Wen Li*[2], *Carol A. Vines*[1] *and James W. Overstreet*[2]
Bodega Marine Laboratory and Department of Environmental Toxicology, and Division of Reproductive Biology, Department of Obstetrics and Gynecology, University of California, Davis, California, USA

Date submitted: 3.11.98. Date accepted: 3.1.99

Summary

The hyaluronic acid (HA)-rich extracellular matrix (ECM) of the cumulus oophorus is known to facilitate fertilisation. It has been suggested that HA may enhance fertilisation in a number of species, and in macaque sperm, HA has been shown to increase the number of acrosome reactions that follow sperm binding to the zona pellucida. In this study, we investigated the effects of HA on intracellular Ca^{2+} in capacitated cynomolgus macaque sperm. Fluorometry studies using the intracellular Ca^{2+} indicator Fluo-3 showed that addition of 100 µg/ml of HA induced a rapid increase in intracellular Ca^{2+}. This Ca^{2+} increase (approximately 2–3 times above basal levels) was inhibited by preincubation of sperm with Fab fragments of anti-recombinant PH-20 IgG. The frequency of acrosome reactions in sperm exposed to HA was not above control levels. A synthetic gel was prepared with similar viscosity to the cumulus and with HA trapped in its matrix. Video imaging of individual sperm was used to demonstrate that capacitated sperm swimming into the HA gel had increased intracellular Ca^{2+} levels. Preincubation of sperm with Fab fragments of anti-PH-20 IgG inhibited the increased intracellular Ca^{2+} levels induced by the HA gel. Sperm in control gel (no HA) did not show increased intracellular Ca^{2+}, while sperm in gel containing anti-PH-20 IgG showed increased Ca^{2+} (positive control). Sperm loaded with Fluo-3 were allowed to interact with cynomologus macaque cumulus masses, and sperm within the cumulus ECM clearly showed increased intracellular Ca^{2+} that was inhibited when sperm were preincubated in anti-PH-20 Fab. Fluorescein isothiocyanate (FITC)-HA was found to bind to sperm over the acrosomal region, corresponding to PH-20 localisation, and this binding could be inhibited by preincubation of sperm with anti-PH-20 fragments. The results of this study show that HA increases intracellular Ca^{2+} in macaque sperm through interaction with plasma membrane PH-20. We propose that HA binding to plasma membrane PH-20 induces an aggregation of receptors that in turn results in intracellular signalling. As a result, sperm have higher basal CA^{2+} levels and are more responsive to induction of the acrosome reaction after binding to the zona pellucida.

Keywords: Cumulus, Hyaluronic acid, PH-20, Sperm signalling

Introduction

The extracellular matrix (ECM) of the cumulus oophorus is secreted by the granulosa cells during follicle maturation and after ovulation (Eppig, 1979; Salustri *et al.*, 1990), a process which has been termed 'mucification' (Dekel & Phillips, 1979). The cumulus ECM is a fibrillar network composed primary of hyaluronic acid (HA) that is extensively cross-linked by protein (Yudin *et al.*, 1988; Cherr *et al.*, 1990; Draharod *et al.*, 1991). This outer investment of the oocyte is a formidable barrier that sperm must traverse prior to contacting the zona pellucida (Cumins & Yanagimachi, 1986; Katz *et al.*, 1986; Cherr *et al.*, 1986; Drobnis *et al.*, 1988; Yudin *et al.*, 1988; reviewed by Yanagimachi, 1994). Sperm motility

All correspondence to: Gary N. Cherr, PO Box 247, Westside Road, Bodega Bay, CA 95616, USA. Tel: +1 (707) 875 2051. e-mail: gncherr@ucdavis.edu
[1]Bodega Marine Laboratory and Department of Environmental Toxicology, University of California Davis, CA 95616, USA.
[2]Division of Reproductive Biology, Department of Obstetrics and Gynecology, University of California, Davis, CA 95616, USA.

is necessary for penetration through the cumulus ECM to the zona surface, and this process requires 3–20 min *in vitro* (Cummins & Yanagimachi, 1982; Cherr *et al.*, 1986; Corselli & Talbot, 1987). Non-capacitated sperm (Cummins & Yanagimachi, 1982, 1986) and sperm that have undergone the acrosome reaction (Suarez *et al.*, 1984; Cherr *et al.*, 1986; Cummins & Yanagimachi, 1986) cannot enter or traverse the cumulus ECM. It is generally accepted that mammalian sperm undergo the acrosome reaction on the surface of the zona pellucida and not within the cumulus (Crozet & Dumont, 1984; Cherr *et al.*, 1986; Drobnis *et al.*, 1988; reviewed by Yanagimachi, 1994), although morphological changes in the acrosomal region of acrosome-intact sperm have been observed during cumulus penetration (Cummins & Yanagimachi, 1986). Cumulus-encased oocytes have higher fertilisation rates than oocytes from which the ECM has been removed (Testart *et al.*, 1983; Chen *et al.*, 1993; reviewed by Yanagimachi, 1994). The mechanism by which the cumulus enhances fertilisation has not been established, although it has been suggested that the cumulus ECM may act as a 'filter' which limits access to the zona pellucida to only those sperm capable of undergoing the acrosome reaction (Cherr *et al.*, 1986).

It is plausible that HA is involved in the mechanisms that regulate sperm function in the cumulus ECM. There are a number of different cell types in which intracellular signalling has been shown to result following the interaction of HA with plasma membrane receptors (Shimizu *et al.*, 1989; Bourguignon *et al.*, 1993; Rao *et al.*, 1996; reviewed by Entwistle *et al.*, 1996). In mammalian sperm, HA has been shown to regulate sperm motility through interaction with specific HA-binding proteins (Kornovsky *et al.*, 1994; Ranganathan *et al.*, 1994), which may be phosphorylated in motile cells (Ranganathan *et al.*, 1994). Most recently, HA has been shown to enhance the zona-induced acrosome reaction in macaque sperm (VandeVoort *et al.*, 1997), and to enhance the progesterone- and zona-induced acrosome reaction in human sperm (Sabeur *et al.*, 1998). In the latter study, HA was shown to increase sperm intracellular calcium concentrations ($[Ca^{2+}]_i$) without inducing acrosome reactions. The glycosylphosphatidylinositol (GPI)-anchored plasma membrane protein PH-20 was shown to be involved in the observed $[Ca^{2+}]_i$ increase, since the increase was inhibited by treatment with Fab fragments of anti-PH-20 IgG (Sabeur *et al.*, 1998). The PH-20 protein is the mammalian sperm hyaluronidase (Gmachl & Kreil, 1993), and in primate sperm PH-20 is located on both the plasma membrane and inner acrosomal membrane (Overstreet *et al.*, 1995; Cherr *et al.*, 1996; Sabeur *et al.*, 1997). There is a putative HA-binding domain in PH-20 that is distinct from the hyaluronidase domain (Gacesa *et al.*, 1994). It is possible that HA-induced aggregation of the PH-20 protein is the stimulus for increased $[Ca^{2+}]_i$, since aggregation of plasma membrane PH-20 following treatment with anti-PH-20 IgG (but not Fab fragments) also causes increased $[Ca^{2+}]$ in macaque sperm (Yudin *et al.*, 1998).

In this study we measured $[Ca^{2+}]_i$ in individual cynomologus macaque sperm during penetration of synthetic gels containing HA, and during interaction with macaque cumulus ECM *in vitro*. The role of plasma membrane PH-20 in HA-induced cell signalling was investigated using Fab fragments of anti-PH-20 IgG. Our results support the model that HA in the cumulus ECM interacts with plasma membrane PH-20 to modulate the function of the sperm acrosome prior to fertilisation.

Materials and methods

Reagents

All the chemicals used in media preparation were purchased from Sigma Chemical Company (St Louis, MO). Caffeine, dbcAMP, digitonin, dimethylsulphoxide, Ficoll, hyaluronic acid and EGTA were also obtained from the Sigma Chemical Company. Fluo-3 AM and Pleuronic F-127 were obtained from Molecular Probes (Eugene, OR). Fluorescein isothiocyanate hydrazide, protein A agarose and a Fab fragment purification kit were purchased from Pierce Scientific (Rockford, IL). The sources for all other reagents are given in the description of specific methods.

Semen collection

Semen samples were collected from male cynomolgus macaques by electroejaculation (Sarason *et al.*, 1991). All animals were housed at the California Regional Primate Research Center in compliance with the Federal Animal Welfare Act and the National Institutes of Health guidelines for Care and Use of Laboratory Animals. Semen samples were held at room temperature for 30 min following collection and were then diluted with 8 ml of a modified Biggers, Whitten and Whittingham (BWW) medium (Overstreet *et al.*, 1980) containing 3 mg/ml of bovine serum albumin (BSA) and 21 mM HEPES buffer (pH 7.4) (HEPES-BWW), and allowed to settle for 15 min. The upper 6 ml of the diluted semen was removed to obtain sperm for washing, and the coagulum was discarded.

Antibody production

A polyclonal antibody (designated '4030') to recombinant PH-20 protein (a gift from Dr Paul Primakoff) was generated in rabbits according to Lin *et al.* (1994). Fifty micrograms of recombinant PH-20 was mixed with Freund's complete adjuvant for the first injection, while

https://doi.org/10.1017/S0967199499000593 Published online by Cambridge University Press

the same amount of protein was mixed with Freund's incomplete adjuvant for the subsequent two injections. All three injections were 2 weeks apart, with the final bleed being 10 days after the last injection. IgG was isolated from serum using Protein A agarose beads followed by elution with a glycine buffer (pH 3.5) and extensive dialysis against phosphate-buffered saline (PBS). Fab fragments were prepared from 4030 IgG using a Fab fragment preparation kit. Dialysed Fab was further purified by subjecting the Fab solution to ultrafiltration using a Centricon (Amicon, Danvers, MA) with a 100 kDa cutoff membrane, with collection of the filtrate.

A polyclonal antibody (designated '4639') was generated to non-denatured macaque sperm plasma membrane PH-20. Sperm surface PH-20 was isolated using glycosylphosphoinositol-specific phospholipase C (PI-PLC; Sigma Chemical Co., St Louis, MO). Sperm were washed in BWW lacking BSA at 400 *g* for 10 min and resuspended in 2 ml of PBS. The sperm suspension was layered onto 40% Percoll in PBS and centrifuged at 400 *g* for 15 min. The pellet was washed twice with 10 ml PBS and resuspended at 100–200 $\times 10^6$/ml. One unit of PI-PLC and protease inhibitors (20 mM EDTA, 1 mM *p*-hydroxymercurobenzenzoate, 5 mM *N*-ethylmaleimide, and 1 mM *para*-amino benzamidine) were then added, and sperm were incubated at 37 °C for 2 h with gentle rolling. Following the PI-PLC incubation, sperm were centrifuged at 3000 *g* and the supernatant stored at –80 °C. Prior to isolation of PH-20 from the supernatant using immunoaffinity chromatography, samples were subjected to ultracentrifugation (100 000 *g* for 1 h) and 0.22 µm filtration.

An immunoaffinity column was generated using 4030 IgG and Actigel-ALD resin (Sterogene, Carlsbad, CA) according to the instructions provided with the resin. Briefly, 4030 IgG (5 mg) in cooling buffer was added to 1 ml of resin and incubated overnight. The resin was then washed and coupling efficiency determined by measuring IgG concentration in the washes. Beads were then washed with 10 volumes of 0.5 M NaCl. The resin was then endcapped by adding 6 ml of coupling buffer, 1 ml ALD-coupling solution and 50 µl of ethanoldiamine and incubated for 2 h. PH-20 was purified from the PI-PLC supernatant in the manner. The affinity gel was pre-washed with elution buffer (50 mM glycine-HCl, pH 2.3). Then 1 M Tris-HCl (pH 8.0) was added immediately to neutralise the beads and they were washed with 10 gel volumes of 50 mM Tris-HCl, pH 7.5, containing 0.025% Triton X-100, 0.025% Tween 20 and 0.3 M NaCl (TTBS). Tween was added to the PI-PLC-proteins (final 0.5%) and the protein solution added to the beads and incubated for 3–5 h at 10 °C. The beads were then centrifuged to remove the supernatant and washed with TTBS 5× (20–30 gel volumes). PH-20 was eluted with 2–3 volumes of elution buffer (8 min incubation with rolling), and the eluant adjusted to pH 8.0 with 1 M Tris-HCl (pH 8.0). PH-20 was concentrated using ultrafiltration (10 kDa cutoff) and purity assessed by 10% sodium dodecyl sulphate polyacrylamide gel electrophoresis (SDS-PAGE) and silver straining. The eluant appeared as a single 64 kDa band on silver-stained gels. The eluant (10 µg) was diluted with complete Freund's adjuvant and injected into rabbits for polyclonal antibody production. Four injections 2 weeks apart (10 µg/injection) were used. IgG and Fab fragments of the 4639 polyclonal antibody were isolated as described above.

Antibody reactivity with denatured whole sperm proteins was conducted using SDS-PAGE followed by immunoblotting as previously described (Li *et al.*, 1997).

Sperm loading with Fluo-3

Sperm were washed twice by centrifugation (300 *g*) and dilution with fresh medium and were resuspended to a concentration of 20 $\times$ 10^6/ml. Washed sperm were stored at room temperature (RT) for a period ranging from 3 to 24 h prior to loading with the intracellular calcium indicator Fluo-3. Preliminary investigation showed no effect of overnight sperm storage on the endpoints being measured in these experiments. Under these storage conditions, sperm are relatively quiescent and become vigorously motile when the medium is warmed to 37 °C. Sperm was loaded with Fluo-3/AM at a concentration of 2.5 µM (from a 1 mM stock solution in 90% DMSO/10% Pleuronic F-127) for 2 h in the dark at RT. Subsequent to loading, sperm suspensions in 500 µl aliquots were layered over equal volumes of either 10% Ficoll in HEPES-BWW or 40% Percoll in HEPES-BWW, and centrifuged for 10 min at 750 *g*. The pellets were pooled and resuspended in 12 ml of HEPES-BWW medium and washed once at 600 *g* for 6 min. The concentrated Fluo-3 loaded sperm (500 µl) were then layered under 3 ml of medium in a conical culture tube, pre-equilibrated at 37 °C, and then incubated at that temperature for 60 min. Highly motile sperm from the top 2 ml of medium were then removed and incubated at 37 °C for an additional 60 min. Samples with less than 70% motile sperm at the end of incubation were discarded. Capacitation was induced by adding 1 mM each of the activators caffeine and dbcAMP and incubating the sperm suspension for an additional 30 min at 37 °C (Vande Voort *et al.*, 1992).

Experimental treatments

Following capacitation, Fluo-3 loaded sperm were treated with human umbilical cord HA (Sigma Chemical Co., St Louis, MO), which was added at a final concentration of 100–200 µg/ml or with 4030 IgG (100 µg/ml final concentration) as a positive control (Yudin *et al.*, 1998). Some sperm aliquots were pretreated with

https://doi.org/10.1017/S0967199499000593 Published online by Cambridge University Press

Fab fragments of the anti-PH-20 IgG addition of HA. Fab fragments (100 µg/ml) of 4030 IgG were added during the last 10 min of chemical capacitation.

Intracellular calcium measurements on sperm suspension in cuvettes

To determine changes in intracellular calcium $[Ca^{2+}]_i$, capacitated, Fluo-3 loaded sperm were diluted into BWW medium at a concentration of $1–5 \times 10^5$/ml and placed in stirred methacrylate cuvettes at 37 °C. The time courses of changes in $[Ca^{2+}]_i$ over 10 min were monitored. A Photon Technology International spectrofluorimeter equipped with a magnetically stirred four-cuvette temperature-controlled turret was used for all $[Ca^{2+}]_i$ measurements. Excitation was at 502 nm and emission was at 536 nm. The response of sperm to 13 µM ionomycin as well as the maximum and minimum fluorescence for each experiment were measured to ensure responses in all treatments were comparable. Maximum fluorescence (R_{max}) was measured following addition of digitonin (50 µM final) to permeabilize cells at the end of the experiment, and minimum fluorescence (R_{min}) was then measured following addition of Tris-buffered 5 mM EGTA (final concentration). Quantitative comparisons between different treatments were measured as the relative differences in fluorescence response between aliquots of sperm treated in the same experiment. The experiment was repeated six times.

Intracellular calcium measurements on individual sperm in synthetic gels

A polyacrylamide gel with viscoelastic properties that slow sperm motility but enable sperm to swim directionally was used to make measurements of $[Ca^{2+}]_i$ on individual sperm cells. The gel has no known physiological effects on sperm, and macaque sperm show no evidence of any change in motility for up to 1 h of incubation in the gel (unpublished data). Polyacrylamide (a gift from Dr Susan Suarez) was used at a 1.5% concentration in BWW with 30 mM sodium bicarbonate and 26 mg/ml BSA. HA (100–200 µg/ml) or 4030 IgG (100 µg/ml final concentration) was incorporated into the polyacrylamide matrix by vortexing and slowly mixing. The gels were aliquoted and frozen at –70 °C until used. For experiments, 20 µl of the HA gel were placed on a slide, 1–2 µl of capacitated, Fluo-3 loaded sperm (with or without 4030 Fab pre-treatment) was added at one side, and the preparation was covered with a coverslip supported by 50 µm glass beads with silicon posts and surrounded by warm mineral oil. Capacitated, Fluo-3 loaded sperm were similarly exposed to gels containing 4030 IgG. The preparations were incubated at 37 °C for 5–10 min, at which time they were removed from the incubator and observed in an Olympus BH-2 upright microscope using interference contrast optics to locate motile sperm that had migrated deeply within the gel. The experiment was repeated four times.

For fluorescence imaging, a 340 nm UV-corrected objective lens was employed. The excitation wavelength (490 nm) was controlled by an automatic filter wheel (Sutter Instruments Lambda-10–2, Novato, CA) in the UV path, while emission wavelength was set at 530 nm using a filter in the interference contrast slider. Integrating Cohu and MTI CCD video cameras were employed, interfaced via a Data Translations framegrabber board to Axon Instruments Workbench 2.1 software (Axon Instruments, Foster City, CA) or a Scion framegrabber through NIH image 1.69 on a Macintosh computer, respectively. All images within a complete experiment were captured under identical conditions with respect to microscope, video camera and software settings so they would be directly comparable. Only sperm with progressive motility that had reached at least 100 µm from the edge of the gels were used for image collection. Sperm were often too active to capture an adequate image immediately, but UV illumination typically slowed or stopped progression within 20 s. For this reason, all images were collected 10–15 s following first illumination with UV light.

Intracellular calcium measurements on individual sperm within the macaque cumulus ECM

Oocyte–cumulus complexes (OCCs) were recovered by ultrasound-guided transabdominal aspiration from superovulated female macaques as described previously (Meyers *et al.*, 1997). OCCs were placed in HEPES-BWW and maintained at 37 °C until used within several hours following collection. OCCs or cumulus ECM fragments from OCCs (< 2 mm diameter) were placed under a coverslip supported by 50 µm glass beads and 0.5–1 µl of capacitated, Fluo-3 loaded sperm (with or without Fab pre-treatment) was added at one side. Slides with sperm–OCC mixtures were incubated at 37 °C for 3 min, and then examined under interference contrast optics. Images were collected over a 15 min period while sperm interacted with the cumulus ECM. Only sperm exhibiting active flagellar movement were imaged. Since sperm progressed much slower in the cumulus than in gels, image capture in the cumulus ECM was easier. However, in order to capture corresponding interference contrast and fluorescence images, sperm were illuminated with UV light for 20 s prior to fluorescence image capture in order to immobilise them for interference contrast imaging. The observations were carried out with sperm from three different males. In some treatments the fluorescence image was overlaid on the interference contrast image using Adobe Photoshop 4.0.

https://doi.org/10.1017/S0967199499000593 Published online by Cambridge University Press

Measurements of HA binding to intact sperm

HA binding to intact sperm was determined based on the procedure of Yu & Toole (1995). Human umbilical HA was fluoresceinated using fluorescein isothiocyanate (FITC)-hydrazide in conjunction with *N*-ethyl-*N*′-(3-dimethylaminopropyl)carbodiimide hydrochloride in a 50 mM borate buffer (pH 5.2) such that approximately 80% of HA carboxyl groups were conjugated with FITC. The reaction was stopped after 18 h by dialysis in 50 mM acetate buffer, followed by extensive dialysis in PBS.

Capacitated sperm were incubated with 50 µg/ml FITC-HA (final concentration in HEPES-BWW) in the presence of the hyaluronidase inhibitor quercitin (200 µM) (Li *et al.*, 1997) for 10 min and then washed two times before fixation. Another aliquot of sperm was pretreated for 10 min in 4030 Fab fragments or 4639 Fab fragments (100 µg/ml) prior to FITC-HA addition. Control sperm were preincubated in unlabelled HA (500 µg/ml) for 10 min, followed by addition of 50 µg/ml FITC-HA. Following the 10 min incubations in FITC-HA, sperm were washed twice in HEPES-BWW (lacking BSA), and the pellets fixed in 90% methanol/10% 50 mM Tris (pH 7.8) at –20 °C for 10 min. Prior to viewing, samples were washed twice in PBS and cells were mounted in an anti-fade medium (90% glycerol/10% PBS with 0.2% *N*-propylgallate). One hundred random sperm from each treatment were counted using an epifluorescence microscope (Olympus BH-2) with a ×60 objective lens using the appropriate FITC excitation and emission filters. Sperm were scored as positive for HA binding if any foci were evident over any region of the sperm head. For image capture, single or Z-series of images were collected digitally using either a scanning laser confocal microscope (Bio-Rad MRC 600) or an Olympus BH-2 epifluorescence microscope equipped as described above. Five representative images from each treatment were collected for image presentation. These experiments were repeated four times.

Assessment of sperm acrosome reactions

The percentage of live acrosome reacted sperm was determined following a 10 min incubation of capacitated sperm in either HEPES-BWW, HEPES-BWW containing 200 µg/ml HA, or HEPES-BWW containing 13 µM ionomycin. Aliquots of the same sperm suspensions were loaded with Fluo-3 and assessed for $[Ca^{2+}]_i$ using a spectrofluorimeter as described above. Acrosome reactions were determined by the method of Cross *et al.* (1986) as modified by Overstreet *et al.* (1995). Bisbenzimide 333258 was added to the sperm suspension (1 µg/ml) during the last 5 min of incubation. Sperm were fixed in 2% formaldehyde in PBS for 10 min, and layered on a PBS/2% polyvinyl pyrrolidone (PVP) solution and centrifuged at 650 *g* for 10 min. The pellet was washed once in PBS and sperm were placed on polylysine-coated slides and allowed to air-dry. Slides were incubated in 100% ethanol for 2 min to permeabilise cells, and processed as described in Overstreet *et al.* (1995) using Texas Red-conjugated *Pisum sativum* agglutinin (Vector Laboratories, Burlingame, CA) (50 µg/ml). One hundred sperm that excluded bisbenzimide 333258 were counted in each sample to determine the percentage of live sperm that were acrosome-reacted. The experiment was repeated three times.

Data analysis

Random images from each experiment were used for quantitation of the region of interest (ROI). All images were inverted and the threshold set to identical levels. For quantitation of pixels, an ROI was designated that represented a circular area the diameter of a sperm head and that was placed as a centroid over each sperm head. The ROI was first calibrated to the black background of each image using the NIH Image optical density calibration macro. Once calibrated, the ROI pixel number per sperm head for all of the sperm from a given treatment were generated. Data from four separate experiments were pooled and the mean and standard deviation determined (Excel 5.0). For each experiment, all data were normalised such that control sperm pixel data represented a pixel value of 1.0; data from experimental treatments were then expressed as a change from a pixel value of 1.0. Since different experiments showed varying magnitudes of response, this was the most conservative method for determining differences between treatments. Data were analysed using the one-tailed Dunnett *t*-test for multiple comparisons between results obtained with different treatments. This test requires that the observations are independent and normally distributed and that variance is homogeneous across all concentrations. A Student's *t*-test was also used to determine whether a specific treatment differed from the control. Values of $p < 0.05$ were considered significant. A two-way ANOVA was used in some experiments to determine whether treatments within an experiment differed.

Results

Antibody specificity

The 4030 anti-recombinant PH-20 antibody (IgG fraction), as well as the 4639 anti-plasma membrane PH-20 antibody (IgG fraction), exhibited similar specificity on western blots to whole non-acrosome-reacted macaque

https://doi.org/10.1017/S0967199499000593 Published online by Cambridge University Press

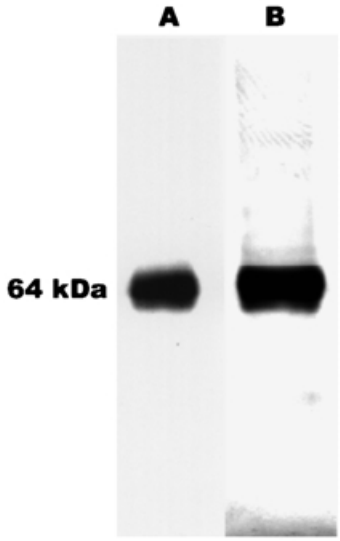

Figure 1 (*A*) Western blot of whole macaque sperm showing specificity of anti-recombinant PH-20 antibody (IgG fraction) 4030. Only the 64 kDa band is labelled. IgG concentration was 10 µg/ml. (*B*) Western blot of whole sperm showing specificity of anti-non-denatured plasma membrane PH-20 antibody (IgG fraction) 4639. Only the 64 kDa band binds the antibody. IgG concentration used was 10 µg/ml.

sperm (Fig. 1*A, B*). Only a 64 kDa band was immunoreactive with both antibodies. In four separate experiments with non-acrosome-reacted macaque sperm, only the 64 kDa band was observed to bind both antibodies.

HA induces an increase in sperm $[Ca^{2+}]_i$

Capacitated macaque sperm exhibited a rapid increase in $[Ca^{2+}]_i$ following exposure to HA or to 4030 IgG (Fig. 2*A*). The rise in $[Ca^{2+}]_i$ was rapid and generally remained above the baseline levels. There was a characteristic decrease in fluorescence following the initial increase, which was observed with all treatments including ionomycin and digitonin (data not shown), and that was probably due to photobleaching of the Fluo-3 probe. The levels of $[Ca^{2+}]_i$ increase (approximately 2–3-fold) in both HA- and 4030 IgG-treated sperm were similar in most experiments. Pre-treatment of sperm with Fab fragments of 4030 IgG (100 µg/ml) prevented the $[Ca^{2+}]_i$ rise induced by HA (Fig. 2*B*). The decrease in fluorescence due to photobleaching of the probe can be seen in the Fab-treated sperm exposed to HA (Fig. 2*B*).

In three experiments in which the percentages of live acrosome-reacted sperm were assessed, the increase in $[Ca^{2+}]_i$ following exposure to HA was similar to that observed in other experiments. The mean percentage of live acrosome-reacted sperm following HA treatment (6.5 ± 1.5) was not significantly different from that of control sperm (5.9 ± 1.9). Following ionomycin treatment, the percentage of acrosome-reacted sperm increased significantly (24 ± 5.9, $p < 0.01$) in comparison with controls.

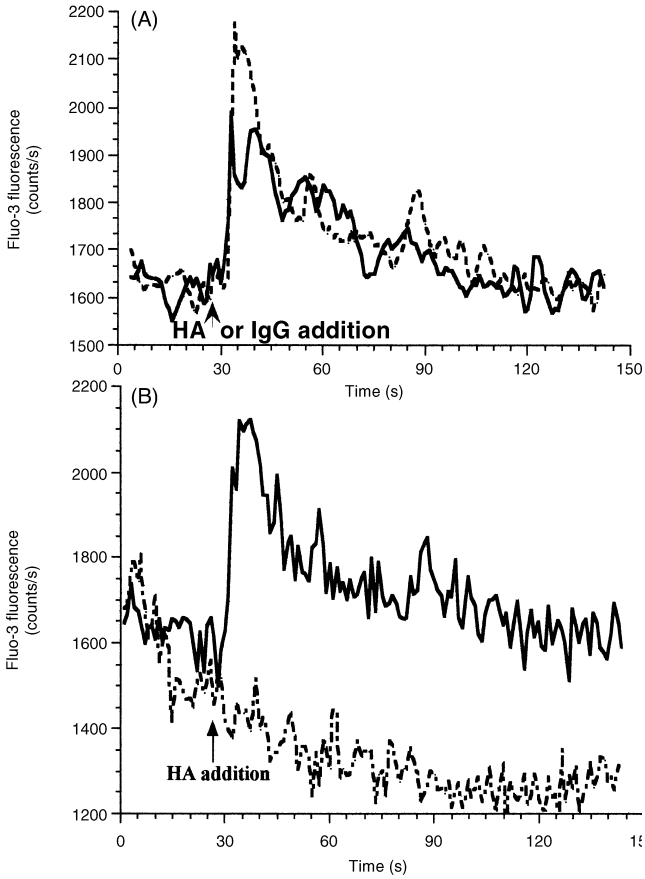

Figure 2 (*A*) Fluo-3 fluorescence of sperm exposed to either 100 µg/ml HA (dashed line) or 100 µg/ml 4030 IgG (continuous line). The $[Ca^{2+}]_i$ increase reaches a maximum that ranges from 2 to 3 times the basal level in capacitated sperm. Traces are from one experiment representative of six similar separate experiments. (*B*) Sperm pretreated with Fab fragments of 4030 IgG (100 µg/ml) (dashed line) do not exhibit the increase in $[Ca^{2+}]_i$ observed in the absence of Fab treatment (continuous line). Although the $[Ca^{2+}]_i$ remains elevated above basal levels when not continuously excited with UV light (not shown), photobleaching results in a decline in fluorescence over time for all treatments.

Sperm in synthetic gels containing HA exhibit $[Ca^{2+}]_i$ increases

Gel preparations typically contained 25 to 75 motile sperm that were at least 100 µm from the edge of the gel. Sperm in gels containing HA exhibited increased Fluo-3 fluorescence compared with sperm in control gels (not shown), and this response was inhibited when sperm were pretreated with Fab fragments of 4030 IgG (Fig. 3). In general, HA-induced fluorescence was observed in the head region and was most obvious in the equatorial and post-acrosomal regions, rather

https://doi.org/10.1017/S0967199499000593 Published online by Cambridge University Press

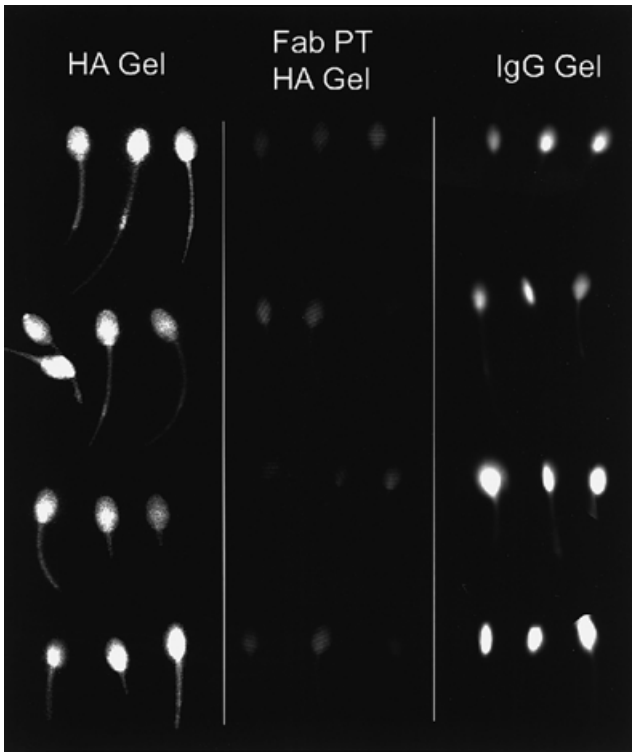

Figure 3 Fluo-3 fluorescence composite of sperm in polyacrylamide gel containing: (1) 100 µg/ml HA ('HA Gel); (2) sperm pretreated with Fab fragments of 4030 IgG (100 mg/ml) in HA gel ('Fab PT HA Gel'); and (3) sperm in gel containing 100 µg/ml 4030 IgG ('TgG Gel'). Note that the greatest fluorescence ($[Ca^{2+}]_i$ increase) is observed over the central portion of the sperm head. Increases in $[Ca^{2+}]_i$ were also observed in the sperm midpiece and flagellum, and may represent global increases or the effect of HA on HA-binding proteins in the tail.

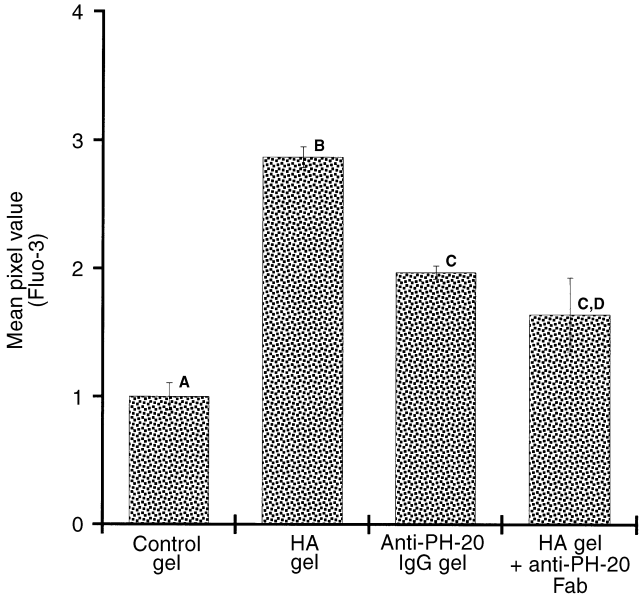

Figure 4 Summary of pixel intensities of sperm in gels ($n = 4$). The values are means of regions of interest (ROIs) over the sperm heads and were normalised to control values at an arbitrary value of 1. The HA gel sperm and the IgG gel sperm were significantly different from control gel sperm ($p < 0.01$ and $p < 0.05$, respectively). Different letters indicate whether a given treatment is significantly different from another. Sperm pretreated with Fab fragments of 4030 IgG in HA gels were significantly different from untreated sperm in HA gels ($p < 0.05$).

than at the anterior margin of the cell. The midpieces of HA-treated sperm also exhibited increased fluorescence (Fig. 3). Sperm in gels containing anti-PH-20 IgG also had increased head fluorescence, but tended to show more variability than those in HA gels (Fig. 3). Individual sperm in the IgG gels clearly showed a higher level of fluorescence than sperm in HA gels.

A summary of the pixel values for the different treatments is shown in Fig. 4. The number of sperm for which images were collected from each treatment within an experiment ranged from 10 to 32. Pixel values of the ROIs from sperm in HA and IgG gels were significantly higher than those in the control gel. Treatment of sperm with Fab fragments of 4030 IgG resulted in a significant decrease in pixel intensity compared with untreated sperm in the HA gel (Fig. 4).

Sperm in macaque cumulus ECM exhibit $[Ca^{2+}]_i$ increases

Sperm entry into the cumulus ECM was much slower than sperm entry into artificial gels. The general behaviour of the sperm traversing the cumulus was very similar to what has been previously described for hamster sperm (Cherr *et al.*, 1986; Yudin *et al.*, 1988; Drobnis *et al.*, 1988). Sperm in the cumulus ECM exhibited Fluo-3 fluorescence in the head region that was blocked when sperm were pretreated with Fab fragments of 4030 IgG (Plate 1, facing p. 218). The number of Fab-treated sperm entering the cumulus ECM appeared to be lower than the number of untreated sperm that entered similar cumulus preparations. There did not appear to be a correlation between distance from the edge of the cumulus and head fluorescence; but differences may have been obscured by the lack of forward progression of many sperm within the cumulus ECM. The mean pixel value for the sperm of three different males in the cumulus ECM was significantly lower when Fab-treated sperm were compared with untreated sperm (Fig. 5).

HA binding to sperm

FITC-HA bound to capacitated sperm over the acrosomal region of the anterior head (Fig. 6*A–D*). The labelling was not always uniform and there was an indication that there were foci of labelling. Sperm in all treatments showed some midpiece fluorescence, and this was considered non-specific. Pretreatment of sperm with Fab fragments of both 4030 and 4639 IgG

https://doi.org/10.1017/S0967199499000593 Published online by Cambridge University Press

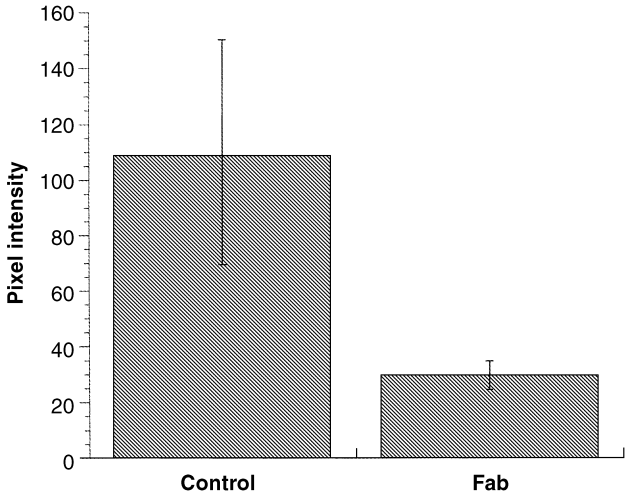

Figure 5 Summary of pixel values for control sperm and sperm pretreated with Fab fragments of 4030 IgG prior to interaction with the macaque cumulus ECM (n = 3). Means were normalised to control sperm values with an arbitrary value of 1. Sperm pretreated with 4030 Fab fragments showed a significant ($p < 0.05$) decrease in Fluo-3 fluorescence compared with controls.

inhibited FITC-HA binding over the sperm head (Fig. 6*C* and *D*, respectively). Sperm preincubated with a 10-fold excess of non-conjugated HA prior to incubation with FITC-HA appeared very similar to sperm preincubated with Fab (Fig. 6*B*). The quantitative results of HA-binding experiments are shown in Table 1. The Fab fragments from the recombinant and non-denatured PH-20 antibodies, as well as non-conjugated HA pretreatment, significantly ($p < 0.001$) inhibited FITC-HA binding to the head of macaque sperm.

Discussion

It is likely that the first sperm that reaches the zona pellucida of the oocyte is destined to be the fertilising sperm *in vivo*. Interactions between the vanguard sperm and the oocyte investments are likely to govern

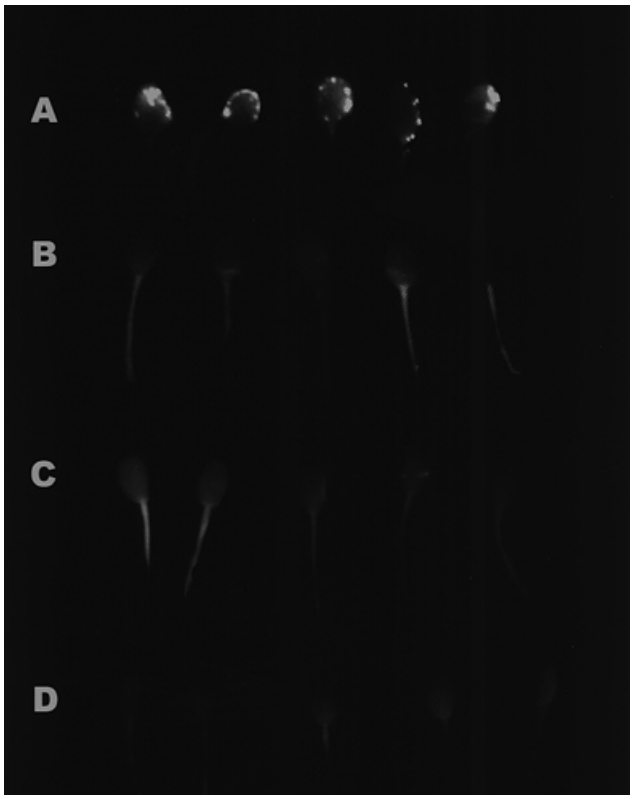

Figure 6 Composite confocal micrographs of FITC-HA binding to capacitated macaque sperm with or without pretreatment with excess non-conjugated HA, Fab fragments of 4030 IgG built against recombinant PH-20, or Fab fragments of the 4639 antibody built against non-denatured plasma membrane PH-20. All incubations in FITC-HA were conducted in the presence of quercitin in order to inhibit hyaluronidase activity so that maximal HA binding could be observed. (*A*) FITC-HA (50 µg/ml) labelled sperm. Note the distinct foci and 'horseshoe' labelling in the second sperm from the left. (*B*) Sperm preincubated in 500 µg/ml non-conjugated HA prior to FITC-HA incubation show a dramatic decrease in sperm with head labelling. (*C*) Sperm preincubated in 100 µg/ml 4030 Fab fragments prior to FITC-HA labelling also show a decreased frequency of head labelling. (*D*) Sperm preincubated in 100 µg/ml 4639 Fab fragments prior to FITC-HA labelling appear similar to 4030 Fab-treated sperm.

Table 1 FITC-HA labelling of capacitated macaque sperm

Treatment	Sperm with head fluorescence (%)
FITC-HA (50 µg/ml)	61.39 ± 1.61
Unlabelled HA (500 µg/ml)+ 50 µg/ml FITC-HA	36.79 ± 5.86*
4030 Fab (100 µg/ml)+ 50 µg/ml FITC-HA	32.83 ± 4.72*
4639 Fab (100 µg/ml)+ 50 µg/ml FITC-HA	39.83 ± 5.08*

Percentages represent means ± standard deviation from four separate experiments.
Activated macaque sperm were preincubated in excess unlabelled HA or Fab fragments for 15 min prior to addition of FITC-HA for 10 min. All samples contained 200 mM quercitin during incubations to inhibit hyaluronidase activity of PH-20.
Sperm were scored as binding AH if labelling was observed over any region of the head as described in Materials and Methods.
*Significant difference from controls (FITC-HA alone) at $p < 0.001$.

https://doi.org/10.1017/S0967199499000593 Published online by Cambridge University Press

the success of fertilisation. The presence of the cumulus has been shown to increase fertilisation rates *in vitro*, suggesting that it also has an important physiological function *in vivo* (reviewed by Yanagimachi, 1994). HA is known to initiate intracellular signalling in other cells (Entwistle *et al.*, 1996). For example, HA has been shown to signal lymphocytes via an HA-bindig protein, with a resulting increase in tyrosine phosphorylation, second messenger (IP_3) formation, and a rise in intracellular calcium (Rao *et al.*, 1996). Previous studies have suggested that both the cumulus and the zona are capable of inducing the acrosome reaction of the fertilising sperm (reviewed by Meizel, 1985). HA has been shown to induce a small increase in acrosome reactions of hamster sperm (Meizel & Turner, 1986), and there is a dramatic enhancement in the acrosome reactions of macaque sperm when they are exposed to HA before binding to the zona pellucida (VandeVoort *et al.*, 1997). Experiments with human sperm have demonstrated a similar potentiating effect of HA on the acrosome reaction induced by either progesterone or solubilised human zona pellucida (Sabeur *et al.*, 1998). The mechanism appears to be mediated by the PH-20 protein since it can be blocked by Fab fragments of anti-PH-20 IgG, and it involves an increase in the basal levels of internal sperm calcium (Sabeur *et al.*, 1998).

This study has shown that HA increases $[Ca^{2+}]_i$ in capacitated macaque sperm without inducing acrosome reactions, and that this increase is comparable to that induced by anti-PH-20 IgG, which appears to act through aggregation of the PH-20 protein (Yudin *et al.*, 1998). We have observed that non-capacitated macaque sperm exhibit a lower $[Ca^{2+}]_i$ level than capacitated sperm, and do not respond to HA (data not shown). This suggests that capacitation is required for the HA-induced $[Ca^{2+}]_i$ increase. The mechanism of the HA-mediated increase in $[Ca^{2+}]_i$ appears also to involve the PH-20 protein since the response was blocked when sperm were treated with Fab fragments of anti-recombinant PH-20 (4030) IgG. The increase in $[Ca^{2+}]_i$ in the present study was observed within 30 s of exposure to HA or 4030 IgG and then $[Ca^{2+}]_i$ declined. This time course differs from what was observed in our previous study with anti-recombinant PH-20 IgG, in which $[Ca^{2+}]_i$ continued to rise throughout a 500 s period of observation (Yudin *et al.*, 1998). Much of this difference can be attributed to the use of Fluo-3 in the present study rather than Fura-2, which was used by Yudin *et al.*. The use of a ratiometric dye such as Fura-2 eliminates photobleaching effects on fluorescence values; such effects were clearly observed in the present study. Nevertheless, the present study demonstrated that HA treatment of macaque sperm resulted in a 2- to 3-fold increase in basal $[Ca^{2+}]_i$ levels compared with the control. This finding is consistent with the increase in $[Ca^{2+}]_i$ observed in human sperm treated with HA (Slotte *et al.*, 1993; Sabeur *et al.*, 1998), as well as the evidence form other cell types that HA induces calcium mobilisation (Bourguignon *et al.*, 1993; Galluzo *et al.*, 1995).

This is the first study to employ an artificial 'ECM' or gel to investigate changes in sperm $[Ca^{2+}]_i$. The polyacrylamide gel used in the present study does not have the elastic properties of the cumulus ECM, but it does have a high viscosity and it is able to trap macromolecules such as IgG and the much higher molecular weight HA. The high viscosity and lack of elasticity of the gel is similar to the properties of the cumulus ECM following protease treatment (Cherr *et al.*, 1990). Sperm were slowed considerably once inside the gel, and it apparently excluded sperm with poor motility. As a consequence, all sperm that penetrated the gel (> 100 μm from the edge) had excellent motility and are likely to be the highest-quality cells within the population. Sperm within gels containing HA or 4030 IgG had increased $[Ca^{2+}]_i$, but it is unlikely that these cells were acrosome-reacted, since cells similarly challenged with HA and IgG in the absence of gels did not undergo acrosome reactions (this study and Yudin *et al.*, 1998). It was interesting to note that non-capacitated sperm could enter these artificial gels but did not show increased $[Ca^{2+}]_i$ (data not shown). The $[Ca^{2+}]_i$ increase in macaque sperm that results from HA exposure appears to be a global increase rather than a focal increase (Florman, 1994), but is clearly most pronounced over the sperm head. Although $[Ca^{2+}]_i$ was increased in the midpiece as a consequence of interaction between HA and PH-20, other HA-binding proteins such as RHAMM and HABP could also be involved, since these proteins are also thought to mediate HA-induced cell signalling events in the sperm midpiece and flagellum (Kornovski *et al.*, 1994; Ranganthan *et al.*, 1994).

Macaque sperm interacted with the cumulus cells and ECM in a manner similar to that reported previously for hamster sperm (Cherr *et al.*, 1986; Yudin *et al.*, 1988; Drobnis *et al.*, 1988). Macaque sperm movements in the cumulus ECM included rapid vibratory motions of the flagella, and periods of extreme lateral head displacement. Typically, these movements were followed by more linear progression through the ECM, after which the non-linear behaviour pattern was repeated. As a consequence, considerable time (10–15 min) was required for the first sperm to reach the zonae pellucidae of oocytes that were 1–2 mm from the site of sperm addition. Such sperm behaviour (lateral head displacement without progressive motility) in the cumulus ECM could be required for effective enzyme action of sperm surface PH-20 in depolymerising the cumulus ECM (Yudin *et al.*, 1988; Thaler & Cardullo, 1995).

https://doi.org/10.1017/S0967199499000593 Published online by Cambridge University Press

The increases in sperm $[Ca^{2+}]_i$ that we observed during cumulus penetration sheds light on older observations of sperm within the cumulus ECM. Cummins & Yanagimachi (1986) reported observations with phase-contrast microscopy that suggested hamster sperm within the cumulous had 'initiated' the acrosome reaction prior to reaching the zona pellucida. These observations included a change in the refractile properties of the sperm head and an apparent swelling of the acrosomal region. However, it was noted that these sperm were not acrosome-reacted. Yudin *et al.* (1988) reported that sperm exposure to anti-recombinant PH-20 IgG underwent acrosomal swelling as well as an increase in $[Ca^{2+}]_i$. Thus, it is possible that HA in the cumulus ECM may induce a similar swelling in the acrosomes of penetrating sperm as a consequence of $[Ca^{2+}]_i$ increases.

In the present study we showed that HA can bind to the head of capacitated macaque sperm, and that PH-20 may be the site of HA binding, since binding was inhibited by treatment with Fab fragments of anti-recombinant as well as non-denatured plasma membrane PH-20 IgG. PH-20 has a putative HA binding region (Gacesa *et al.*, 1994) that is rich in basic amino acids and has two regions of repeating basic amino acids (within the region of amino acids #205–235). These repeating basic amino acids are characteristic of HA binding proteins (Peach *et al.*, 1993),and have been shown to be involved in HA interaction with plasma membrane receptors for the HA molecule. The binding of HA to proteins involves divalent interactions, and when the molecular weight of HA is higher, the binding affinity is stronger (Tamoto *et al.*, 1993). Such differences in binding affinity have functional implications, since there is increased inhibition of chemotactic activity in polymorphonuclear leucocytes when cells are exposed to higher molecular weight HA (Tamoto *et al.*, 1994). It has been suggested that a single molecule of high molecular weight HA ($> 10^6$ Da) can cross-link numerous cell surface receptors, and that this cross-linking is responsible for specific intracellular signalling (Tamoto *et al.*, 1994). While we have not conducted ultrastructural studies of HA binding to the macaque sperm head, our fluorescent confocal images suggest that HA may not be evenly distributed over the acrosomal region but rather is often bound in discrete foci; some of these sperm appear to possess a 'horseshoe'-shaped labelling pattern along the leading edge of the sperm (see Fig. 6*A*) as described by Yudin *et al.* (1998). While this appearance could be due to a number of experimental artifacts (methanol fixation, presence of quercitin, etc.), this observation is also consistent with a mechanism in which HA cross-links PH-20 and thereby induces cell signalling and increased $[Ca^{2+}]_i$.

GPI-anchored proteins are known to be involved with increases in $[Ca^{2+}]_i$ and tyrosine phosphorylation when they are aggregated by ligands or multivalent antibodies (Morgan *et al.*, 1993; reviewed by Brown, 1993). PH-20 moves rapidly within the plasma membrane (Myles & Primakoff, 1984; Yudin *et al.*, 1998) and this movement probably occurs when it binds its substrate, HA (Thaler & Cardullo, 1995). While binding of HA is likely to be a required event for hydrolysis, the putative enzymatic site is approximately 50 amino acids away from the HA binding site and toward the N-terminus of the protein (between amino acids 148 and 168; Arming *et al.*, 1997). The active site of hyaluronidase is thought to have an acidic amino acid residue(s) that acts as a nucleophile for the acid–base catalyst reaction and this site is also known to have a base or charged region to aid in substrate binding. This whole region is flanked by aromatic amino acids such as tryptophan and/or tyrosine (Withers & Aebersold, 1995). We speculate that there is only limited HA hydrolysis as a result of plasma membrane PH-20 interaction with the cumulus ECM, and that the high concentrations of macromolecular HA in the cumulus ECM provide a source of HA for continuous binding to PH-20 in the HA binding region.

It is likely to that HA binding to PH-20 resulted in the activation of Ca^{2+} channels. It is now believed that sperm-specific 'T-type' Ca^{2+} channels are present in mouse sperm, and are activated when sperm contact the zona pellucida (Arnoult *et al.*, 1996, 1997; Lievano *et al.*, 1996). While these channels are inhibited by dihydropyridines, they have been classified as T-type channels due to their electrophysiological characteristics and their inhibition by Ni^{2+} and Co^{2+}. These channels are voltage-dependent (via membrane depolarisation) and are modulated by tyrosine phosphorylation during fertilisation (Arnoult *et al.*, 1997). We have observed that the HA-induced increase in $[Ca^{2+}]_i$ is not inhibited by dihydropyridines or Ni^{2+} (unpublished observations), indicating that the $[Ca^{2+}]_i$ channels involved in the HA response are different from those involved in the zona-pellucida-induced acrosome reaction. The results of the present study are consistent with the hypothesis that increases in $[Ca^{2+}]_i$ that result from interactions between PH-20 and HA involve a different mechanism from the one that mediates zona-pellucida-induced $[Ca^{2+}]_i$ increases. Such a dichotomy would explain the inability of HA alone to induce acrosome reactions (VandeVoort *et al.*, 1997; Sabeur *et al.*, 1998; this study) as well as the lack of acrosome reactions in sperm treated with anti-PH-20 IgG (Yudin *et al.*, 1998).

In conclusion, the present study has provided evidence that HA within the cumulus ECM modulates the $[Ca^{2+}]_i$ of macaque sperm as they approach the zona pellucida. Our experiments suggest that the mecha-

https://doi.org/10.1017/S0967199499000593 Published online by Cambridge University Press

nism of this action involves HA binding to the PH-20 protein on the sperm surface. These findings are consistent with our model that HA in the cumulus ECM primes the fertilising sperm to undergo the acrosome reaction after binding to the zona pellucida.

Acknowledgements

The authors are grateful to Dr Susan Suarez for her generous gift of polyacrylamide used in this study and to Ms Katy Robertson and Dr Mary Scott for preparation of sperm samples. The authors also thank Dr Paul Primakoff for his generous gift of the recombinant PH-20 which was used to generate a polyclonal antibody in this study and Dr Catherine VandeVoort for supplying the macaque OCCs. This work was supported by NIH U54-HD29125 and NIH P51-RR00169, the Andrew W. Mellon Foundation, with partial support from the University of California Toxic Substances Research and Teaching Program.

References

Arming, S., Strobl, B., Wechselberger, C. & Kreil, G. (1997). *In vitro* mutagenesis of PH-20 hyaluronidase from human sperm. *Eur. J. Biochem.* **247,** 810–14.

Arnoult, C., Cardullo, R.A., Lemos, J.R. & Florman, H.M. (1996). Activation of mouse sperm T-type Ca^{++} channels by adhesion to the egg zona pellucida. *Proc. Natl. Acad. Sci. USA* **93,** 13004–9.

Arnoult, C., Lemos, J.R. & Florman, H.M. (1997). Voltage-dependent modulation of T-type calcium channels by protein tyrosine phosphorylation. *EMBO J.* **16,** 1593–9.

Bourguignon, L.Y.W., Lokeshwar, V.B., Xia, C., Kerrick, W. & Genn, L. (1993). Haluronic acid-induced lymphocyte signal transduction and HA receptor (GP85/CD44) cytoskeleton interaction. *J. Immunol.* **15,** 6634–44.

Brown, D. (1993). The tyrosine kinase connection: how GPI-anchored proteins activate T cells. *Curr. Opin. Immunol.* **5,** 349–54.

Chen, L., Russel, P.T. & Larsen, W.J. (1993). Functional significance of cumulus expansion on the mouse: roles for the preovulatory synthesis of hyaluronic acid within the cumulus mass. *Mol. Reprod. Dev.* **34,** 87–93.

Cherr, G.N., Lambert, H., Meizel, S. & Katz, D.F. (1986). *In vitro* studies of the golden hamster acrosome reaction: completion on the zona pellucida and induction by homologous soluble zonae pellucidae. *Dev. Biol.* **114,** 119–31.

Cherr, G.N., Yudin, A.I. & Katz, D.F. (1990). Organization of the hamster cumulus extracellular matrix: a hyaluronate–glycoprotein gel which modulates sperm access to the oocyte. *Dev. Growth Differ.* **32,** 353–65.

Cherr, G.N., Meyers, S.A., Yudin, A.I., VandeVoort, C.A., Myles, D.G., Primakoff, P. & Overstreet, J.W. (1996). The PH-20 protein in cynomologus macaque spermatozoa: identification of two different forms exhibiting hyaluronidase activity. *Dev. Biol.* **175,** 142–53.

Corselli, J. & Talbot, P. (1987). *In vitro* penetration of hamster oocyte–cumulus complexes using physiological numbers of sperm. *Dev. Biol.* **122,** 227–42.

Cross, N.L., Morales, P.M., Overstreet, J.W. & Hanson, F.W. (1986). Two simple methods for detecting acrosome-reacted human sperm. *Gamete Res.* **15,** 213–26.

Crozet, N. & Dumont, M. (1984). The site of the acrosome reaction during *in vivo* penetration of the sheep oocyte. *Gamete Res.* **10,** 97–105.

Cummins, J.H. & Yanagimachi, R. (1982). Sperm–egg ratios and the site of the acrosome reaction during *in vivo* fertilization in the hamster. *Gamete Res.* **5,** 239–56.

Cummins, J.H. & Yanagimachi, R. (1986). Development of ability to penetrate the cumulus oophorus by hamster spermatozoa capacitated *in vitro* in relation to the timing of the acrosome reaction. *Gamete Res.* **15,** 187–212.

Dekel, N. & Phillips, D.M. (1979). Maturation of rat cumulus oophorus: a scanning electron microscopy study. *Biol. Reprod.* **21,** 9–18.

Drahorad, J., Tesarik, J. & Cechova, D. (1991). Proteins and glycosaminoglycans in the intercellular matrix of the human cumulus oophorus and their effect on conversion of proacrosin to acrosin. *J. Reprod. Fertil.* **93,** 252–62.

Drobnis, E.Z., Yudin, A.I., Cherr, G.N. & Katz, D.F. (1988). The kinematics of hamster sperm during penetration of the cumulus cell matrix. *Gamete Res.* **21,** 367–83.

Entwistle, J., Hall, C.L. & Turley, E.A. (1996). HA receptors: regulators of signalling to the cytoskeleton. *J. Cell Biochem.* **61,** 569–77.

Eppig, J.J. (1979). FSH stimulates hyaluronic acid synthesis by oocyte–cumulus cell complexes from mouse preovulatory follicles. *Nature* **281,** 483–4.

Florman, H.M. (1994). Sequential focal and global elevations of sperm intracellular Ca^{++} are initiated by the zona pellucida during the acrosomal exocytosis. *Dev. Biol.* **165,** 152–64.

Gacesa, P., Civill, N.D. & Harrison, R.A.P. (1994). PH-20 and sperm hyaluronidase: a conceptual conundrum in mammalian fertilization. *Biochem. J.* **303,** 335–6.

Galluzo, E., Albi, N., Fiorucci, S., Merigola, C., Ruggeri, L., Tosti, A., Grossi, C.E. & Velardi, A. (1995). Involvement of CD44 variant isoforms and hyaluronate adhesion by human activated T cells. *Eur. J. Immunol.* **30,** 2932–9.

Gmachl, M. & Kreil, G. (1993). Bee venom hyaluronidase is homologous to a membrane protein of mammalian sperm. *Proc. Natl. Acad. Sci. USA* **90,** 3569–73.

Hunnicutt, G.R., Mahan, K., Lathrop, W.F., Ramarao, C.S., Myles, D.G. & Primakoff, P. (1996). Structural relationship of sperm soluble hyaluronidase to the sperm membrane protein PH-20. *Biol. Reprod.* **54,** 1343–9.

Katz, D.F., Cherr, G.N. & Lambert, H. (1986). The evolution of hamster sperm motility during capacitation and interaction with the ovum vestments *in vitro*. *Gamete Res.* **14,** 333–46.

Kornosky, B.S., McCoshen, J., Kredentser, J. & Turley, E. (1994). The regulation of sperm motility by a novel hyaluronan receptor. *Fertil. Steril.* **61,** 935–40.

Li, M.-W., Cherr, G.N., Yudin, A.I. & Overstreet, J.W. (1997). Biochemical chararcterization of the protein on the plasma and inner acrosomal membrane of cynomolgus macaque spermatozoa. *Mol. Reprod. Dev.* **48,** 356–66.

Lievano, A., Santi, C.M., Serrano, C.J., Trevino, C.L., Bellve, A.R., Hernandez-Cruz, A. & Darzon, A. (1996). T type Ca^{++} channels and α_{1E} expression in spermatogenic cells, and their possible relevance to the sperm acrosome reaction. *FEBS Lett.* **388,** 150–4.

Lin, Y., Mahan, K., Lathrop, W.F., Myles, D.G. & Primakoff, P. (1994). A hyaluronidase activity of the sperm plasma membrane protein PH-20 enables sperm to penetrate the cumulus cell layer surrounding the egg. *J. Cell Biol.* **125,** 1157–63.

Meizel, S. (1985). Molecules that initiate or help stimulate the acrosome reaction by their interaction with the mammalian sperm surface. *Am. J. Anat.* **174,** 285–302.

Meizel, S. & Turner, K.O. (1986). Glycosaminoglycans stimulate the acrosome reaction of previously capacitated hamster sperm. *J. Exp. Zool.* **237,** 137–9.

Meyers, S.A., Yudin, A.L., Cherr, G.N., VandeVoort, C.A., Myles, D.G., Primakoff, P. & Overstreet, J.W. (1997). Hyaluronidase activity of *in vitro* capacitated macaque sperm assessed by *in vitro* cumulus penetration assay. *Mol. Reprod. Dev.* **46,** 392–400.

Morgan, B.P., van den Berg, C.W., Davies, E.V., Hallett, M.B. & Horejsi, V. (1993). Cross-linking of CD59 and of other glycosyl phosphatidylinositol-anchored molecules on neutrophils triggers cell activation via tyrosine kinase. *Eur. J. Immunol.* **23,** 2841–50.

Myles, D.G. & Primakoff, P. (1984). Localized surface antigens of guinea pig sperm migrate to new regions prior to fertilization. *J. Cell Biol.* **99,** 1634–41.

Overstreet, J.W. Lin, Y., Yudin, A.I., Meyers, S.A., Primakoff, P., Myles, D.G., Katz, D.F. & VandeVoort, C.A. (1995). Location of the PH-20 protein on acrosome-intact and acrosome-reacted spermatozoa of cynomologus macaques. *Biol. Reprod.* **52,** 105–14.

Overstreet, J.W., Yanagimachi, R., Katz, D.F., Hayashi, K. & Hanson, F.W. (1980). Penetration of human spermatozoa into the human zona pellucida and zona-free hamster egg: a study of fertile donors and infertile patients. *Fertil. Steril.* **33,** 534–42.

Peach, R.J., Hollenbaugh, D., Stamenkovic, I. & Aruffo, A. (1993). Identification of hyaluronic acid binding sites in the extracellular domain of CD44. *J. Cell Biol.* **122,** 257–64.

Rao, C.M., Deb, T.B. & Datta, K. (1996). Hyaluronic acid induced hyaluronic acid binding protein phosphorylation and inositol triphosphate formation in lymphocytes. *Biochem. Mol. Biol. Int.* **40,** 327–37.

Ranganathan, S., Ganguly, A.K. & Datta, K. (1994). Evidence for presence of hyaluronan binding protein on spermatozoa and its possible involvement in sperm function. *Mol. Reprod. Dev.* **38,** 69–76.

Sabeur, K., Cherr, G.N., Yudin, A.I., Primakoff, P., Li, M. & Overstreet, J.W. (1997). The PH-20 protein in human spermatozoa. *J. Androl.* **18,** 151–8.

Sabeur, K.S., Cherr, G.N., Yudin, A.I. & Overstreet, J.W. (1998). Hyaluronic acid enhances induction of the acrosome reaction of human sperm through interaction with the PH-20 protein. *Zygote* 6, 103–11.

Salustri, A., Yanagishita, M. & Hascall, V. (1990). Mouse oocytes regulate hyaluronic acid synthesis and mucification by FSH-stimulated cumulus cells. *Dev. Biol.* **138,** 26–32.

Sarason, R.L., VandeVoort, C.A., Mader, D.R. & Overstreet, J.W. (1991). The use of nonmetal electrodes in electroejaculation of restrained by unanesthetized macaques. *J. Med. Primatol.* **20,** 122–5.

Shimizu, Y., Van Seventer, G.A., Siraganian, R., Wahl, L. & Shaw, S. (1989). Dual role of the CD44 molecule in T cell adhesion and activation. *J. Immunol.* **143,** 2457–63.

Slotte, H., Akerlof, E. & Pousette, A. (1993). Separation of human spermatozoa with hyaluronic acid induces, and Percoll inhibits, the acrosome reaction. *Int. J. Androl.* **16,** 349–54.

Suarez, S.S., Katz, D.F. & Meizel, S. (1984). Changes in motility that accompany the acrosome reaction in hyperactivated hamster spermatozoa. *Gamete Res.* **10,** 253–65.

Tamoto, K., Tada, M., Shiamda, S., Nochi, H. & Mori, Y. (1993). Effects of high molecular weight hyaluronates on the functions of guinea pig polymorphic leukocytes. *Semin. Arthritis Rheum.* **22** (Suppl 1): 4–8.

Tamoto, K., Nochi, H., Tada, M., Shimada, S., Mori, Y., Kataoka, S., Suzuki, Y. & Nakamura, T. (1994). High-molecular weight hyaluronic acids inhibit chemotaxis and phagocytosis but not lysosomal enzyme release induced by receptor-mediated stimulations in guinea pig phagocytes. *Microbiol. Immunol.* **38,** 73–80.

Testart, J., Mendoza, C., Moos, J., Fenichel, P. & Fehlmann, M. (1983). A study of factors affecting the success of human fertilization *in vitro.* I. Influence of ovarian stimulation upon the number and condition of oocytes collected. *Biol. Reprod.* **28,** 415–25.

Thaler, C.D. & Cardullo, R.A. (1995). Biochemical characterization of a glycosyl-phosphatidylinositol-linked hyaluronidase on mouse sperm. *Biochemistry* **34,** 7788–95.

VandeVoort, CA., Tollner, T.L. & Overstreet, J.W. (1992). Sperm–zona pellucida interaction in cynomolgus and rhesus macaques. *J. Androl.* **13,** 428–32.

VandeVoort, C.A., Cherr, G.N. & Overstreet, J.W. (1997). Hyaluronic acid enhances the zona pellucida-induced acrosome reaction of macaque sperm. *J. Androl.* **18,** 1–5.

Withers, S.G., & Aebersold, R. (1995). Approaches to labeling and identification of active site residues in glycosidases. *Prot. Sci.* **4,** 361–72.

Yanagimachi, R. (1994). Mammalian fertilization. In *The Physiology of Reproduction*, ed. E. Knobil & J.D. Neill, pp. 189–317. New York: Raven Press.

Yu, Q. & Toole, B.P. (1995). Biotinylated hyaluronan as a probe for detection of binding proteins in cells and tissues. *BioTechniques* **19,** 122–9.

Yudin, A.I., Cherr, G.N. & Katz, D.F. (1988). Structure of the cumulus matrix and zona pellucida in the golden hamster: a new view of sperm interaction with oocyte-associated extracellular matrices. *Cell Tissue Res.* **251,** 555–64.

Yudin, A.I., Cherr, G.N., VandeVoort, C.A. & Overstreet, J.W. (1988). Rearrangement of the PH-20 protein on the surface of macaque spermatozoa following exposure to anti-PH-20 antibodies or binding to zona. *Mol. Reprod. Dev.* **50,** 207–20.